JOC The Journal of Organic Chemistry

Article

pubs.acs.org/joc

Determining the Absolute Configuration of Two Marine Compounds Using Vibrational Chiroptical Spectroscopy

Kathrin H. Hopmann,*[,†,‡] Jaroslav Šebestík,[§] Jana Novotná,[∥] Wenche Stensen,[#] Marie Urbanová,[⊥] Johan Svenson,[†] John Sigurd Svendsen,[†,#] Petr Bouř,*[,§] and Kenneth Ruud[†,‡]

[†]Department of Chemistry and [‡]Centre for Theoretical and Computational Chemistry, University of Tromsø, N-9037 Tromsø, Norway

[§]Institute of Organic Chemistry and Biochemistry, Academy of Sciences, Flemingovo nám. 2, 166 10 Prague, Czech Republic

[∥]Department of Analytical Chemistry and [⊥]Department of Physics and Measurement, Institute of Chemical Technology, Technická 5, 166 28 Prague, Czech Republic

[#]Lytix Biopharma AS, Tromsø Research Park, N-9294 Tromsø, Norway

Supporting Information

ABSTRACT: Chiroptical techniques are increasingly employed for assigning the absolute configuration of chiral molecules through comparison of experimental spectra with theoretical predictions. For assignment of natural products, electronic chiroptical spectroscopies such as electronic circular dichroism (ECD) are routinely applied. However, the sensitivity of electronic spectral parameters to experimental conditions and the theoretical methods employed can lead to incorrect assignments. Vibrational chiroptical methods (vibrational circular dichroism, VCD, and Raman optical activity, ROA) provide more reliable assignments, although they, in particular ROA, have been little explored for assignments of natural products. In this study, the ECD, VCD, and ROA chiroptical spectroscopies are evaluated for the assignment of the absolute configuration of a highly flexible natural compound with two stereocenters and an asymmetrically substituted double bond, the marine antibiotic Synoxazolidinone A (SynOxA), recently isolated from the sub-Arctic ascidian *Synoicum pulmonaria*. Conformationally averaged nuclear magnetic resonance (NMR), ECD, Raman, ROA, infrared (IR) and VCD spectral parameters are computed for the eight possible stereoisomers of SynOxA and compared to experimental results. In contrast to previously reported results, the stereochemical assignment of SynOxA based on ECD spectral bands is found to be unreliable. On the other hand, ROA spectra allow for a reliable determination of the configuration at the double bond and the ring stereocenter. However, ROA is not able to resolve the chlorine-substituted stereogenic center on the guanidinium side chain of SynOxA. Application of the third chiroptical method, VCD, indicates unique spectral features for all eight SynOxA isomers in the theoretical spectra. Although the experimental VCD is weak and restricted by the limited amount of sample, it allows for a tentative assignment of the elusive chlorine-substituted stereocenter. VCD chiroptical analysis of a SynOxA derivative with three stereocenters, SynOxC, results in the same absolute configuration as for SynOxA. Despite the experimental challenges, the results convincingly prove that the assignment of absolute configuration based on vibrational chiroptical methods is more reliable than for ECD.

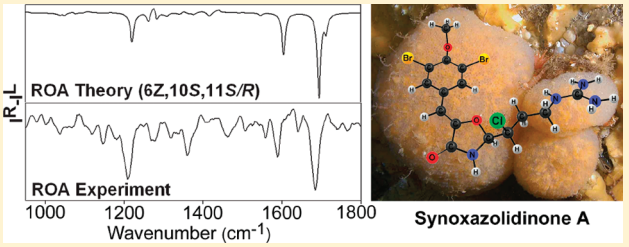

INTRODUCTION

Bioprospecting is a powerful strategy for discovery and isolation of new bioactive natural compounds.[1] However, biological or therapeutical applications of natural products are dependent on a full molecular characterization, including the assignment of the absolute configuration (AC) of chiral compounds. Knowledge about the stereochemical properties is essential for a detailed understanding of the biological activity and is a prerequisite for developing synthetic strategies for the molecule of interest or for more stable derivatives with similar biological functioning. Assignment of the AC based on X-ray crystal structures is the most reliable method (although not completely without failures[2,3]); however, this technique is often time-consuming and is dependent on the ability to form suitable crystals. An alternative and perhaps even more laborious method uses chemical correlation, implying transformation of the molecule of interest into a compound with known stereochemical configuration.[4] Clearly, methods for AC assignment that can be applied immediately to isolated natural products in solution are preferable, in particular if the isolated compounds are only available in limited amounts, as is often the case for natural products. NMR spectroscopic methods are routinely applied for compounds with certain classes of functional groups, including Mosher's method for secondary alcohols,[5,6] and the database method by Kishi.[7] However, the

Received: August 1, 2011
Published: December 12, 2011

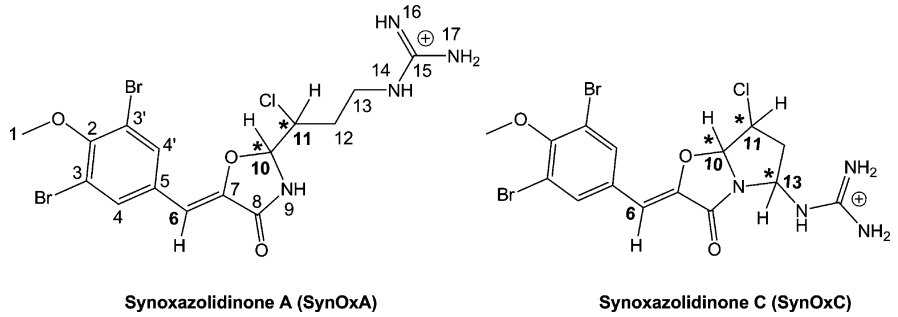

Figure 1. Synoxazolidinones A and C (chiral centers are marked with asterisks).

diverse range of natural products includes many compounds where these methods are not applicable. The assignment of AC employing electronic chiroptical techniques has emerged as one viable approach, in particular optical rotation (OR, rotation of plane-polarized light passing through a chiral sample) and electronic circular dichroism (ECD, the differential absorption of left and right circularly polarized light in the UV−vis region) have been applied for stereochemical assignments of numerous natural compounds.[8−13] However, OR and ECD spectra usually do not contain many distinct features and are very sensitive to both temperature and solvent,[14,15] which can result in incorrect AC assignments. To obtain a correlation between the sign of a given spectral band and the absolute configuration of a given molecule, assignments increasingly rely on a comparison of experimental spectra to theoretical calculations. This makes the results vulnerable to approximations employed in the computational scheme, including the level of theory, the treatment of environmental effects (such as solvent interactions), and the treatment of molecular flexibility. Both OR and ECD parameters are very sensitive to conformation, and even small changes in the conformer distribution can result in a sign change of the calculated OR and ECD signals.[11,16−23] For larger molecules, the modeling of OR and ECD parameters is typically restricted to TD-DFT methods, which do not provide a systematic way to increase the accuracy of excitation energies and transition dipole moments.[24−26]

The newer vibrational optical activity (VOA) methods offer complementary chiroptical information, as they probe vibrational transitions within the electronic ground state. VOA techniques include Raman optical activity (ROA, which refers to differential intensities of Raman-scattered right and left circularly polarized visible light)[27−30] and vibrational circular dichroism (VCD, which measures the differential absorption of left and right circularly polarized infrared light).[31,32] ROA and VCD spectra involve a larger number of vibrational transitions and are predicted more reliably with current DFT methods than electronic properties.[33] Although VCD and ROA spectra are conformationally dependent, small structural changes usually affect only a limited spectral region and do not lead to a sign change of all spectral bands, as might occur for ECD and OR.[14] VOA spectroscopies are thus increasingly being employed for the assignment of AC, and numerous successful examples have been reported,[33−35,37,38] including AC reassignments wrongly predicted on the basis of ECD or X-ray spectroscopy.[2,16,36−38]

The extensive information provided by VOA is particularly important for complex natural molecules with multiple stereocenters. VOA AC assignments of natural products have mostly relied on VCD analyses,[33,37,38] whereas ROA techniques mainly have been applied to synthetic molecules, often with restricted conformational flexibility (less than five conformations), and/or involving a single stereocenter only.[34,39−41] On the other hand, ROA has been extensively used to study conformation and secondary structure of amino acids, peptides and carbohydrates.[42−50] Two rare examples of AC studies of natural compounds employing ROA are assignment of a single stereocenter in the monoterpenoid Junionone from *Juniperus communis*[35] and assignment of two stereocenters in the antiangiogenic compound Aeroplysinin 1 from *Aplysina cavernicola*.[51] However, for the latter case, the computed spectral signs of the enantiomers were not opposite, indicating that the assignment may not be reliable.[51] The applicability of ROA techniques for AC assignments of natural products is thus little explored.

Here we report a combined experimental and theoretical study to determine the AC of a novel antibacterial and antifungal compound, Synoxazolidinone A (SynOxA, Figure 1), recently isolated from the sub-Arctic ascidian *Synoicum pulmonaria* collected off the coast of Norway.[52] SynOxA has two stereocenters (at C-10 and C-11) and one asymmetrically substituted double bond (between C-6 and C-7), giving a total of eight possible stereoisomers. NMR coupling constants indicated that the most likely configuration at the double-bond is (*Z*).[52] Comparison of the experimental ECD spectrum with theoretical results (LDA/SVP on MD-generated conformers) resulted in a proposed (6*Z*,10*S*,11*S*) stereochemistry for SynOxA.[52] However, the computed ECD spectrum providing the best fit with experiment originated from the (6*E*,10*S*,11*S*)-isomer (and not (6*Z*,10*S*,11*S*)),[53] in conflict with the NMR results.

Two additional synoxazolidinones have been isolated from *Synoicum pulmonaria*: SynOxB, which is similar to SynOxA but lacks the chlorine atom at C-11,[52] and SynOxC, which displays a bicyclic structure formed through a covalent bond between C-13 and N-9 (Figure 1).[54] These compounds likely follow the same metabolic stereoselective pathway. SynOxC has three stereocenters, C-10, C-11 and C-13, the first two of which were assigned to be (10*S*,11*S*), in analogy to SynOxA, whose ECD spectrum is similar to that of SynOxC.[54] A misassignment of the configuration of SynOxA would thus have been passed on to SynOxC. SynOxC exhibits both antibacterial and anticancer activities, but its future use, as that of SynOxA, may depend on an accurate AC assignment.

In order to shed light on the absolute configuration of the synoxazolidinones and to test the applicability of different chiroptical spectroscopies for assignments of flexible natural products in solution, we have performed a combined experimental and theoretical study of SynOxA and SynOxC. For SynOxA, we have measured the Raman, ROA, IR, and VCD spectra and compared them to theoretically generated

dx.doi.org/10.1021/jo201598x | J. Org. Chem. 2012, 77, 858−869

Table 1. Computed[a] and Experimental[b] ^{1}H and ^{13}C NMR Chemical Shifts (ppm, relative to TMS) and $^3J_{C,H}$ Coupling Constant (Hz) for SynOxA; For Atom Labelling, See Figure 1

atom no.	theory δ_H	exptl δ_H	error δ_H	theory δ_C	exptl δ_C	error δ_C
1	3.90 (4.1)	3.87	0.03 (0.27)	62.9 (64.0)	61.2	1.7 (2.8)
2				162.6 (162.6)	154.3	8.3 (8.3)
3/3′				143.9 (145.4)	119.0	24.9[d] (26.4)
4/4′	8.09 (8.38)	7.85	0.24 (0.53)	140.8 (141.3)	134.0	6.8 (7.3)
5				139.6 (140.3)	133.9	5.7 (6.4)
6	6.31 (6.81)	6.06	0.25 (0.75)	109.5 (110.2)	100.6	8.9 (9.6)
7				153.6 (154.6)	146.2	7.4 (8.4)
8				171.0 (172.2)	164.7	6.3 (7.5)
9	5.93 (10.39)	10.2[c]	−4.27 (0.19)			
10	5.92 (6.25)	5.90	0.02 (0.35)	95.8 (98.1)	90.5	5.3 (7.6)
11	4.38 (4.82)	4.38	0.00 (0.44)	74.8 (77.2)	62.3	12.5[d] (14.9)
12	2.31 (2.62)	2.30	0.01 (0.32)	35.8 (37.7)	32.3	3.5 (5.6)
	2.14 (2.39)	1.98	0.16 (0.41)			
13	3.56 (3.93)	3.58	−0.02 (0.35)	44.5 (44.9)	39.3	5.2 (5.6)
14	4.70 (7.23)	8.0[c]	−3.30 (−0.77)			
15				160.7 (163.1)	158.8	1.9 (4.3)
16/17	4.88 (7.38)	7.4[c]	−2.52 (−0.02)			

	theory $^3J_{C,H}$	exptl $^3J_{C,H}$	error $^3J_{C,H}$
$^3J_{C\text{-}8,H\text{-}6}$	3.7	<3	>0.7

[a]Boltzmann average over 36 conformers ($CPCM_{BS1}$) of the *ZSR* isomer (values in parentheses are averaged over 30 cluster conformers), [b]Measured at 600 MHz (^{1}H) and 150 MHz (^{13}C) in CD_3OD and DMSO-d_6.[52] [c]Only seen in DMSO-d_6.[52] [d]These carbons bear halogen substituents (Br or Cl).

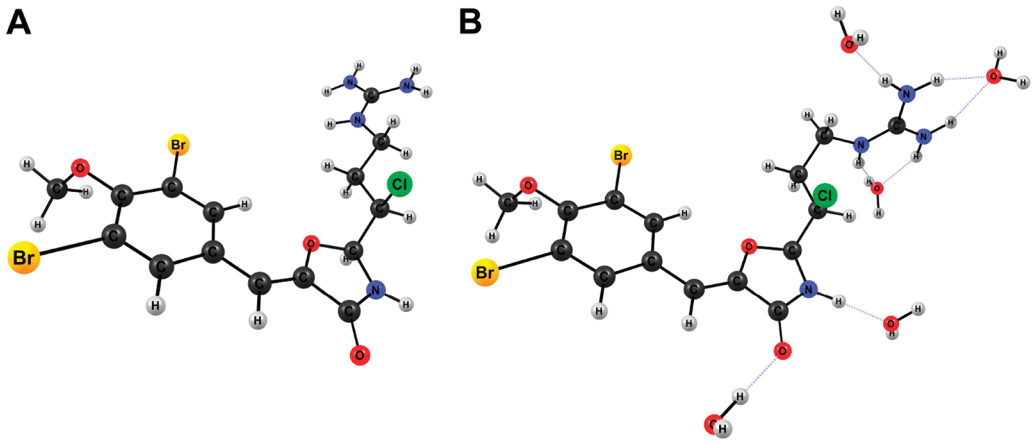

Figure 2. Examples of optimized geometries of the *ZSR* isomer of SynOxA: (A) a $CPCM_{BS1}$ geometry and (B) a cluster geometry with five explicit water molecules.

conformer-averaged spectra for the eight possible stereoisomers. In addition, ECD spectra and NMR properties were computed to verify previous experimental and theoretical results.[52] For SynOxC, we report the experimental and theoretical IR and VCD spectra and compare theoretical ECD spectra to previous experimental results.[54] Our results highlight the strength of VOA techniques over electronic chiroptical spectroscopies and show the necessity of thorough conformational sampling and high-level computational techniques for reliable stereochemical assignments.

RESULTS AND DISCUSSIONS

Geometry Optimizations of SynOxA. There are eight possible stereoisomers of SynOxA, here abbreviated as *ESS*, *ERR*, *ESR*, *ERS*, *ZSS*, *ZRR*, *ZSR*, and *ZRS* (where, e.g., *ZSS* = 6*Z*,10*S*,11*S*). All isomers were optimized quantum mechanically at the B3LYP/6-31+G(d,p)/CPCM level of theory ($CPCM_{BS1}$ geometries). Analysis of the potential energy surfaces revealed 36 local minima with relative enthalpies within 1.5 kcal/mol. For each isomer, all 36 conformers were therefore taken into account in calculations of the spectral properties. To evaluate the effect of different computational approaches on the resulting spectra, we reoptimized the geometries for the (*Z*)-isomers employing (i) a larger basis set (6-311++G(d,p)), referred to as $CPCM_{BS2}$ geometries, (ii) empirical dispersion corrections, referred to as CPCM-D_{BS2} geometries, and (iii) explicit solvation, referred to as cluster geometries (see Methods for further details).

Nuclear Magnetic Resonance Studies of SynOxA. The structure of SynOxA was elucidated empirically on the basis of NMR results,[52] and it is therefore important to verify it by theoretical predictions. We have computed the NMR chemical shifts and selected coupling constants for the different stereoisomers of SynOxA. Only the NMR parameters for the *ESR* and *ZSR* isomers are discussed in the following, as the

dx.doi.org/10.1021/jo201598x | J. Org. Chem. 2012, 77, 858−869

parameters of the other isomers do not provide additional information.

The ^{1}H chemical shifts computed for the *ZSR* isomer are in a good agreement with experiment. For nonacidic hydrogens, theoretical and experimental shifts differ by 0.00−0.25 ppm for values recorded in CD_3OD (Table 1). For acidic protons (H-9, H-14, H-16/17), the shifts could not be measured in CD_3OD because of the exchange with deuterium and were instead measured in DMSO-d_6.[52] For these hydrogens, larger deviations occur in comparison to theory, between −2.52 and −4.27 ppm (Table 1). These chemical shifts are computed using the $CPCM_{BS1}$ geometries, which underestimate the bond length of polar hydrogens in solution, because interactions with the solvent are only partially accounted for by the CPCM model. Indeed, inclusion of explicit water molecules in the model (Figure 2) provides markedly improved chemical shifts for acidic hydrogens (Table 1, values in parentheses), reducing their errors to 0.19 ppm for H-9, −0.77 ppm for H-14, and −0.02 ppm for H-16/H17. These results are in agreement with previously reported environmental effects on NMR parameters.[55] For ^{13}C chemical shifts, the errors are between 1.7 and 8.9 ppm for carbon atoms without halogen substituents. The bromide- and chloride-substituted carbons show larger errors of, respectively, 24.9 and 12.5 ppm, which could be due to lack of relativistic effects in our calculations.[56,57]

For the *ESR* isomer, the computed ^{1}H and ^{13}C NMR values are similar to those for *ZSR*, with the exception of H-4/4′ and C-6. In *ESR*, one of the H-4 hydrogens is positioned close to the C═O of the oxazolidinone ring, giving rise to a larger chemical shift and therefore an increased error of 0.83 ppm (compared to 0.24 ppm for *ZSR*, Supporting Information, Table S1). For C-6, the ^{13}C shift has an error of 18.7 ppm for *ESR* (Supporting Information, Table S1) compared to 8.9 ppm for *ZSR* (Table 1). The larger deviations for the (*E*)-isomer suggest a (*Z*)-configuration for SynOxA, but the differences are not significant enough for a conclusive assignment.

The double bond geometry of SynOxA has previously been addressed in an EXSIDE experiment, which recorded a coupling constant between H-6 and C-8 of $^{3}J_{C,H}$ < 3 Hz.[52] On the basis of literature values for *cis* (*Z*) and *trans* (*E*) double bonds (of respectively 7.6 and 14.1 Hz),[58] the configuration at the double bond was predicted to be (*Z*).[52] Here we have computed the H-6 and C-8 $^{3}J_{C,H}$ coupling constants for the SynOxA isomers and obtained averaged values of 3.7 Hz for *ZSR* (Table 1) and 7.9 Hz for *ESR* (Table S1, Supporting Information). Comparison to the experimental value (<3 Hz) indicates that SynOxA indeed exhibits a (*Z*)-conformation at the double bond.

Electronic Circular Dichroism Spectra of SynOxA. On the basis of the experimental ECD spectrum and computed results at the TD-LDA/SVP level of theory (on MD conformers), the configuration of SynOxA has been suggested to be *ZSS*[52] (or *ESS*[53]). Therefore, for comparison to previous results, we have computed the spectra for all eight SynOxA isomers at the TD-LDA/SVP/CPCM level of theory (Supporting Information, Figure S1), averaged over 36 conformers for each isomer. Additionally, we used the more advanced TD-B3LYP/6-311++G(d,p)/CPCM level (Figure 3, $CPCM_{BS1}$ geometries). Analysis of the computed electronic excitations reveals that the maximum peak in each spectrum (at 317 nm for (*Z*)-conformers and 330 nm for (*E*)-conformers, B3LYP) originates from a HOMO−LUMO $\pi \rightarrow \pi^*$ transition

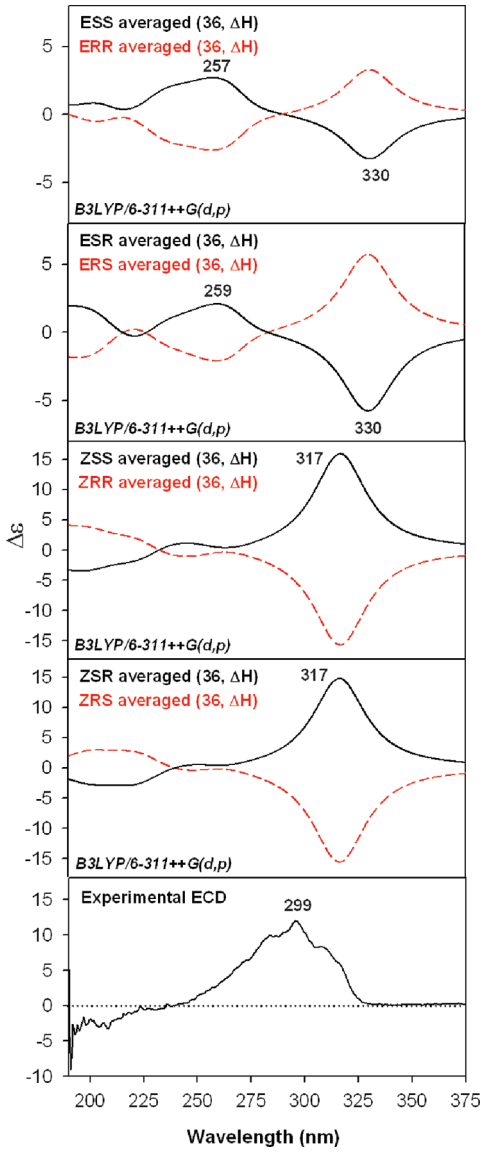

Figure 3. Computed ECD spectra for the eight isomers of SynOxA at the TD-B3LYP/6-311++G(d,p)/CPCM(methanol) level of theory (averaged over 36 conformers for each isomer, bandwidth = 30 nm, *SS*/*SR* isomers are shown with black solid line, *RR*/*RS* isomers with red dashed line). The experimental spectrum is from ref 52.

involving the conjugated Ph−C═C−C═O system of SynOxA (Supporting Information, Figure S2).

The two levels of theory, TD-LDA and TD-B3LYP, result in similar spectral features (Supporting Information, Figure S1). However, the main transitions obtained at the higher (TD-B3LYP) level of theory are blue-shifted by ∼20−40 nm compared to the TD-LDA-based results. These results highlight the well-known dependence of the ECD spectral properties on the level of approximation[23,59] and indicate that comparison to experiment should be done with caution. Such a peak shift can have significant consequences on the interpretation of ECD spectra, as has been observed for the natural products Plumericin and Isoplumericin, for which semiempirical ECD calculations resulted in an incorrect AC assignment,[60] whereas B3LYP-based calculations revealed that unambiguous AC assignments on the basis of ECD spectra are not possible.[37]

dx.doi.org/10.1021/jo201598x | J. Org. Chem. 2012, 77, 858−869

A comparison between previously reported MD/TD-LDA-based ECD results[52] and the QM/TD-LDA spectra computed here show some similarities, with the main peak (centered between 296 and 357 nm, Supporting Information, Figure S1) being of the same sign and similar wavelength as in the previous study (see Supporting Information of ref 52; note that the labeling of spectra therein is incorrect[53]). However, in contrast to the previous study, we find that the chiral center at C-11 of SynOxA is silent in the ECD spectra, resulting in virtually the same pattern for epimers such as *ZSS* and *ZSR* (Supporting Information, Figure S1). This is indicated both by the TD-LDA (Supporting Information, Figure S1) and the TD-B3LYP computations (Figure 3). These results contradict the previously reported MD/TD-LDA-based ECD predictions[52] and show that discrimination between the eight SynOxA isomers on the basis of their ECD spectra is impossible. The discrepancy is likely due to the fact that the previous spectra were based on five MD conformers extracted from the same trajectory with "*little change in the conformations*"[52] and therefore possibly only representing one main conformation. The spectra computed here take into account for each isomer 36 distinct low-energy conformers obtained by a systematic search and are thus far more reliable. These results emphasize the importance of adequate exploration and sampling of the complete conformational space.

The experimental ECD spectrum of SynOxA has only one broad positive peak at ~299 nm (Figure 3, bottom),[52] which makes comparison to theory inconclusive. The peak shape suggests an underlying vibrational structure; this is, however, weak, and its interpretation goes beyond the goal of our study. The ECD spectra computed at the TD-B3LYP/6-311++G(d,p)/CPCM level indicate that the *ZSR* and *ZSS* isomers have one main peak with a maximum at 317 nm, and thus provide relatively good fits with experiment, assuming a red-shift of 20 nm compared to the experimental position. However, the *ERS* and *ERR* isomers, with main positive peaks at 330 nm, might provide reasonable fits as well. We therefore conclude that the experimental and theoretical ECD spectra can rule out four of the eight possible isomers, but are unable to provide detailed information on the stereochemistry of SynOxA. Similar difficulties in determining the AC of compounds with multiple stereocenters have also been observed for Ascolactone, a natural product isolated from the marine-derived fungus *Ascochtya salicorniae*.[13] Ascolactone exhibits two chiral centers, one on the lactone ring, and a second on a substituent. The latter stereocenter is silent in modeled ECD spectra, as observed for C-11 of SynOxA here.

Raman Optical Activity Spectra of SynOxA. In order to shed light on the absolute configuration of SynOxA, we proceeded to analyze the experimental and theoretical Raman and ROA spectra. The theoretical spectra were computed at the B3LYP/6-311++G(d,p)/CPCM level of theory for all eight isomers ($CPCM_{BS1}$ geometries). The conformationally averaged theoretical Raman spectrum of the *ZSR* isomer of SynOxA and the experimental spectrum are shown in Figure 4. The agreement is very good, with reproduction of the intense peaks at 1206, 1586, and 1684 cm^{-1} in the experimental spectrum. These bands are assigned to C−H bending (1206 cm^{-1}, in particular H-4/4′, H-6, H-10, and H-11), aromatic C−C stretching (1586 cm^{-1}, involving C-4 and C-4′), and C═O and C═C stretching (1684 cm^{-1}, involving C-6, C-7, and C(═O)-8). Also in the lower wavenumber region, the theoretical and experimental spectra show very good agreement, with

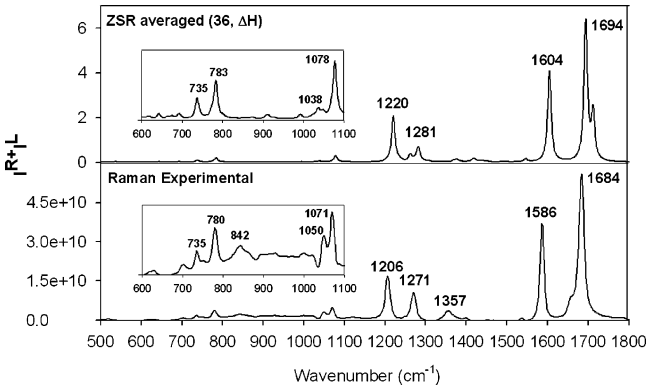

Figure 4. Computed Raman spectrum for the *ZSR* isomer (averaged over 36 conformers, bandwidth = 20 cm^{-1}, top) and the experimental Raman spectrum (bottom). Insets show enlargement of the spectral parts between 600 and 1100 cm^{-1}.

reproduction of the less intense peaks at 735, 780, and 1071 cm^{-1} (Figure 4, inset).

The theoretical ROA spectra for the four (*Z*)-isomers of SynOxA show strong signature bands for the configuration at the C-10 center, with intense negative peaks at 1220, 1604, and 1694 cm^{-1} for (*S*) configurations (*ZSS* and *ZSR*) and positive peaks for (*R*) configurations (*ZRR* and *ZRS*, Figure 5). Thus,

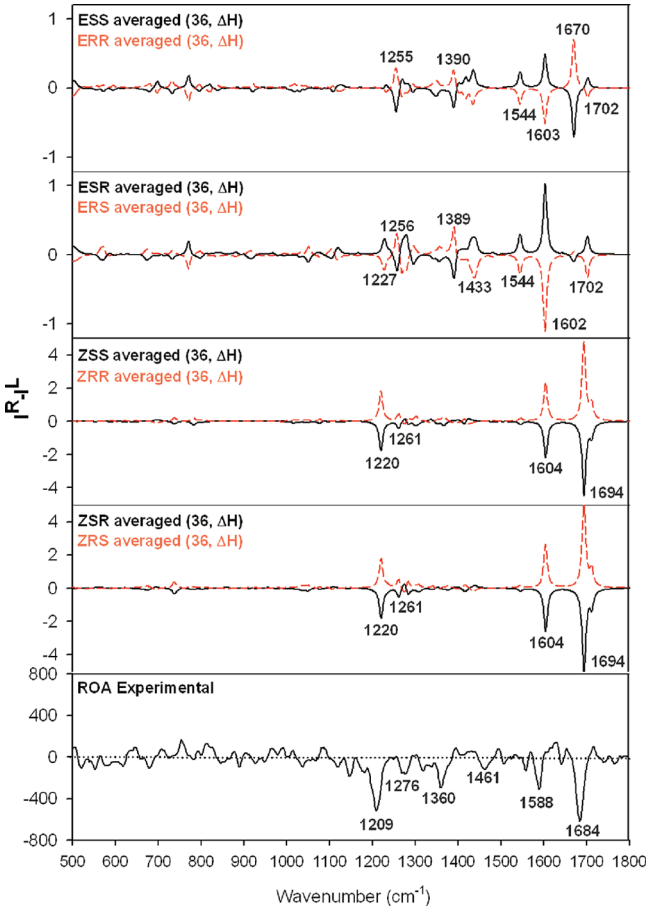

Figure 5. Experimental ROA spectrum (bottom) and the computed ROA spectra for the 8 stereoisomers of SynOxA (averaged over 36 conformers, bandwidth =10 cm^{-1}, *SS*/*SR* isomers are shown with black solid line, *RR*/*RS* isomers with red dashed line).

dx.doi.org/10.1021/jo201598x | J. Org. Chem. 2012, 77, 858−869

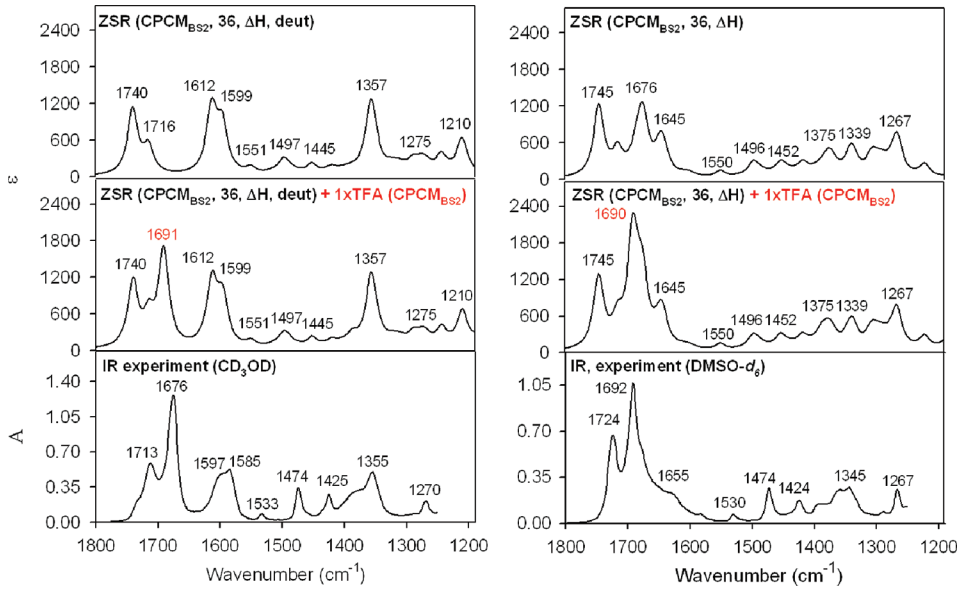

Figure 6. IR spectra in CD_3OD (left) and DMSO-d_6 (right) of SynOxA and computed spectra for the *ZSR* isomer (averaged over 36 conformers, bandwidth 20 cm^{-1}, spectrum in CD_3OD corrected for deuterium exchange) without (top panel) and with TFA spectrum added (middle panel).

the configuration at C-10 of the (*Z*)-isomers can easily be deduced from the ROA spectra. However, the second chiral center at C-11 is silent, making the ROA spectra for *ZSS* and *ZSR* indistinguishable. For the (*E*)-isomers, the *ESS*/*ERR* and *ESR*/*ERS* pairs display somewhat different ROA spectra. The *ESR*/*ERS* spectra show one intense peak at 1602 cm^{-1} and several less intense peaks at 1227, 1389, 1433, 1544, and 1702 cm^{-1} (Figure 5). The main peaks in the *ESS*/*ERR* spectra have similar wavenumbers but show a different intensity pattern. It might thus be possible to differentiate between all four (*E*)-isomers on the basis of their relative ROA intensities. An interesting geometrical effect on the ROA spectra of the (*E*)-isomers concerns the methoxy substituent on C-1: although this group is not chiral and is positioned far away from the chiral center at C-10, its relative orientation (∼−90° or ∼+90° for the C(1)−O−C(2)−C(3) torsional angle) results in a change of the sign for the peaks at ∼1603 and ∼1670 cm^{-1}. For example, for *ERR*, the 18 conformers with ∼−90° have positive peaks (++), whereas the 18 conformers with ∼+90° have negative peaks (− −) for these two bands. The ∼−90° and ∼+90° conformers are close in energy, but their spectral bands have different intensities, implying that they only partially cancel out in the averaged spectrum, resulting in the characteristic (− +) pattern seen in Figure 5 (top panel). A similar ROA contribution of a seemingly optically inactive tryptophan residue has been observed previously.[61] These results highlight the importance of including geometrical effects of groups distant from the chiral centers in ROA analyses.

The experimental ROA spectrum of SynOxA exhibits several intense negative peaks at 1209, 1360, 1588, and 1684 cm^{-1} (Figure 5, bottom panel). These peaks seem to be reliable and are reproducible in independent measurements, despite the noise in the measured spectrum (an example of the raw ROA signal can be seen in Supporting Information, Figure S3). Unfortunately, weaker ROA peaks could not be measured due to limited instrument sensitivity, the tiny amount of the compound, limited solubility, and sample fluorescence. The wave numbers and the relative intensities of the negative peaks at 1209, 1588, and 1684 cm^{-1} show good agreement with the theoretical spectra of the *ZSS* and *ZSR* isomers (assuming a downward shift of the predicted frequencies by ∼10 cm^{-1}, Figure 5). The (*E*)-isomers show poor agreement with the experimental spectrum, confirming the (*Z*)-configuration at the double bond, in agreement with NMR results. Further, on the basis of the recorded and computed ROA spectra, we conclude that the absolute configuration at C-10 of SynOxA is (*S*). The second stereocenter at C-11 cannot be deduced, because the theoretical ROA spectra for the two epimers *ZSS* and *ZSR* exhibit essentially identical spectral features (Figure 5).

The reliable assignment of both the double bond and the C-10 configuration of SynOxA clearly makes ROA preferable over the ECD method. On the other hand, the inability to assign the C-11 center indicates some limitations of ROA. The theoretical results show that on the basis of the ROA intensities (but not the ECD results), individual assignments of both the C-10 and C-11 stereocenters would be possible for the (*E*)-isomers of SynOxA but not the (*Z*)-isomers, indicating that the applicability of ROA for AC assignments of all stereocenters is dependent on the molecular structure. It is interesting that in a similar ROA application employing the synthetic diastereomeric compound Galaxolide as a test case, Hug and co-workers showed that it should be possible to individually assign its two stereocenters (positioned on different rings) on the basis of differences in the theoretical ROA spectra of the possible isomers; however, this awaits experimental conformation.[62]

Vibrational Circular Dichroism of SynOxA. Previous assignments of absolute configurations of natural products using VOA techniques have mainly relied on use of VCD,[33,37,38] and we have therefore also analyzed the experimental and theoretical VCD spectra of SynOxA in order to shed further light on the stereochemistry of this compound. The IR and VCD spectra of SynOxA were recorded in two different solvents, CD_3OD (which causes an exchange of acidic protons with deuterium) and DMSO-d_6 (which does not result in SynOxA deuteration, as verified also by NMR studies[52]).

The recorded IR spectrum of SynOxA in CD_3OD is compared to the averaged theoretical spectrum in Figure 6

dx.doi.org/10.1021/jo201598x | J. Org. Chem. 2012, 77, 858−869

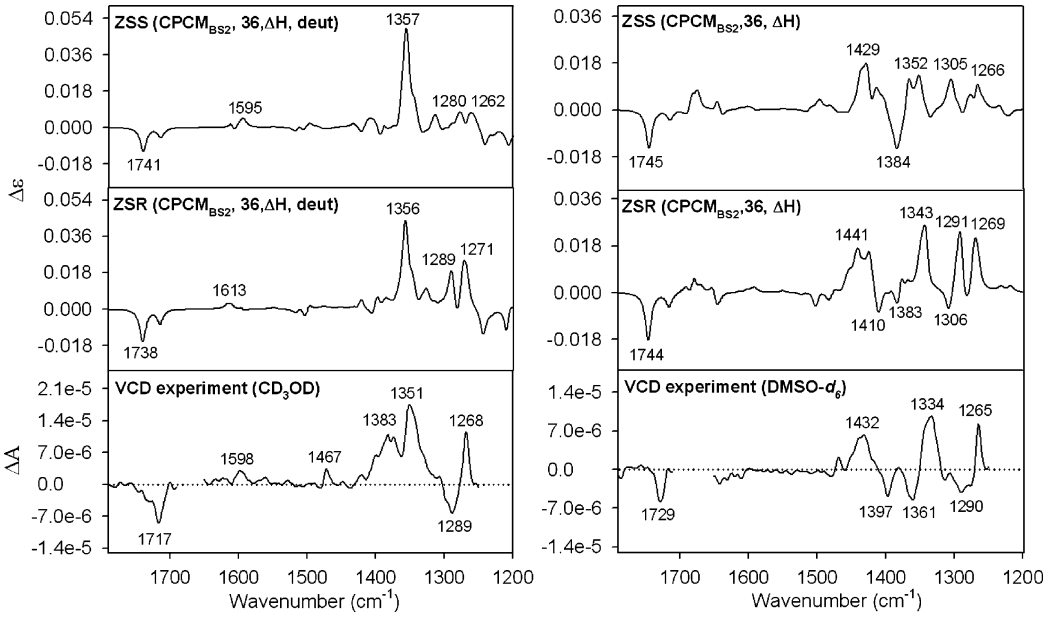

Figure 7. Computed VCD spectra for the *ZSR* and *ZSS* isomers of SynOxA (averaged over 36 conformers, bandwidth 10 cm^{-1}) and the experimental spectra in CD_3OD (left) and DMSO-d_6 (right). The regions around 1650−1710 cm^{-1} in the experimental spectrum in DMSO-d_6 and 1650−1690 cm^{-1} in the spectrum in CD_3OD were omitted because of high noise level.

(left, top panel, the theoretical spectrum was calculated for deuterium exchange at all acidic positions). The main peaks in the theoretical spectrum are assigned to C═O stretching at 1740 cm^{-1}, aromatic C−C stretching at 1612 cm^{-1}, and C−H and N−H/D bending at 1357 cm^{-1} (in particular H-6, H-9, and H/D-10). Comparison to the experimental spectrum shows that the main features are reproduced, however, the intense experimental peak at 1676 cm^{-1} is not found in the theoretical spectrum. This peak is expected to originate from the SynOxA counterion, trifluoroacetic acid (TFA). Indeed, combination of the theoretical SynOxA spectrum with the computed TFA spectrum (Figure 6, middle panel) provides an improved fit with experiment.

The experimental IR spectrum in DMSO-d_6 (Figure 6, right, bottom panel) shows slightly different features than the spectrum in CD_3OD, with the main peaks around 1600 to 1700 cm^{-1} shifted to higher wave numbers. The theoretical IR spectrum without deuterium exchange (Figure 6, right, top panel) reproduces the main spectral features of the spectrum in DMSO-d_6, in particular if it is corrected for the presence of TFA (Figure 6, right, middle panel).

The theoretical VCD spectra for the (*E*)-isomers of SynOxA show little agreement with the experimental spectra in CD_3OD and DMSO-d_6 (Supporting Information, Figures S4 and S5). The theoretical VCD spectra for the four (*Z*)-isomers are shown in Figure S6, Supporting Information. On basis of the ROA results above, SynOxA is expected to exhibit a *ZSR* or *ZSS* configuration, and we therefore concentrate on the VCD spectra for these two isomers (Figure 7). The *ZSR* spectrum with deuterium exchange (Figure 7, left, middle panel) shows three main peaks, 1356, 1289, and 1271 cm^{-1}, all of which originate from C−H bending (mainly H-10, H-11, H-12, H-13), with the 1356 cm^{-1} band also containing significant N−H/D bending. The *ZSS* isomer shows similar peaks (Figure 7, left, top panel), but with different relative intensities than *ZSR*. The theoretical spectra without deuterium exchange exhibit rather different features, with main peaks at 1441, 1343, 1291, and 1269 cm^{-1} for the *ZSR* isomer (Figure 7, right, middle panel). The main peaks for the *ZSS* isomer have similar wave numbers (Figure 7, right, top panel), but different relative intensities than *ZSR*. These results indicate that it could be possible to differentiate between the *ZSS* and *ZSR* isomers on the basis of their VCD spectra, depending on the accuracy of both the experimental and calculated spectra.

The experimental VCD spectra for SynOxA in CD_3OD and DMSO-d_6 could not be measured reliably in the carbonyl stretching region around 1650 to 1700 cm^{-1} (Figure 7, bottom panels). Despite this limitation, good agreements between the experimental and theoretical VCD spectra in the remaining regions are observed. For the spectrum in CD_3OD, both the *ZSS* and *ZSR* isomers exhibit spectral features that fit with the experimental spectra, in particular the bands at 1717, 1351, and 1268 cm^{-1} (Figure 7, left). For these bands, the relative intensities indicate a better fit with the computed VCD spectrum of *ZSR* than that of *ZSS*. The prominent band at 1383 cm^{-1} in the experimental CD_3OD spectrum could not be reproduced (reproduction of this band might require explicit solvent, see below). The calculated 1289 cm^{-1} positive band (*ZSR* isomer) might be assigned to the weaker experimental feature at ∼1300 cm^{-1}. Note that the most intense bands in the theoretical VCD spectra (1356, 1289, and 1271 cm^{-1} for *ZSR*) are mainly originating from C−H bending, which are challenging to model accurately, possibly due to high state density and anharmonicities.[40]

The recorded VCD spectrum in DMSO-d_6 shows different spectral features than the spectrum in CD_3OD, with main bands at 1729, 1432, 1334, and 1265 cm^{-1} (Figure 7, right). The theoretical spectra for both *ZSR* and *ZSS* reproduce all the main bands; however, the *ZSR* isomer provides a significantly better fit, in particular for the relative intensities. The *ZSR* calculated negative peak at 1410 cm^{-1} can be assigned to the 1397 cm^{-1} negative experimental band, whereas the *ZSS* isomer provides a positive signal here. Around 1305 cm^{-1}, the calculated VCD is positive for *ZSS* and negative for *ZSR*.

dx.doi.org/10.1021/jo201598x | *J. Org. Chem.* 2012, 77, 858−869

Since in the experiment there is a negative signal at 1290 cm^{-1}, the *ZSR* isomer provides a better fit, although the positive calculated band at 1291 cm^{-1} is not observed. This inconsistency can be at least partially explained by analysis of the calculated rotational strengths, which revealed vibrations close in frequency and opposite in sign in this region.

As the details of the VCD spectra are rather sensitive to the molecular geometry, we have tested the effect of the basis set used in geometry optimizations and the influence of explicit solvent molecules on the resulting spectra. For the *ZSR* isomer, the spectra computed on the basis of deuterated $CPCM_{BS1}$, $CPCM_{BS2}$, and cluster geometries (with 5 explicit water molecules,[63] Figure 2) are compared in Figure 8. The computed spectra for the $CPCM_{BS1}$ and $CPCM_{BS2}$ geometries display only small differences, with the main difference a shift of

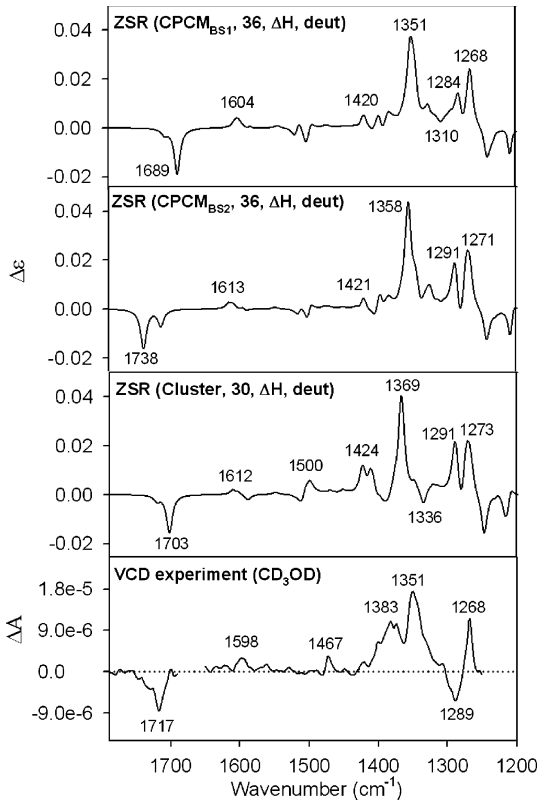

Figure 8. Computed VCD spectra for the *ZSR* isomer of SynOxA with geometry optimization at different levels of theory ($CPCM_{BS1}$, $CPCM_{BS2}$, and cluster geometries) and the experimental spectrum in CD_3OD. The region around 1650−1690 cm^{-1} in the experimental spectrum was omitted because of high noise level.

the 1689 cm^{-1} band to 1738 cm^{-1}. The cluster spectrum shows a shift for the main peak (to 1369 cm^{-1}) and slightly different features in the 1400−1500 cm^{-1} region, providing a slightly improved fit with experiment (Figure 8). The band at 1424 cm^{-1} is more intense in the cluster spectrum, indicating that this might correspond to the 1383 cm^{-1} peak in the CD_3OD experiment. The spectra without deuteration (Supporting Information, Figure S7) also show a limited basis set effect and a more pronounced effect of the explicit solvation. In this case, the spectrum based on cluster geometries provides less agreement with the experimental spectrum in DMSO-d_6 than the $CPCM_{BS2}$ spectrum. This is understandable, as the explicit water molecules employed in the cluster calculations likely provide a better model of the CD_3OD solvent than of the DMSO-d_6 solvent. For the *ZSS* isomer, similar basis set and solvation effects were obtained as for *ZSR* (Supporting Information, Figure S8). Again, a significantly intensified band is obtained at 1414 cm^{-1} in the deuterated *ZSS* cluster spectrum, providing a better description of the 1383 cm^{-1} band observed in the CD_3OD experiment. However, the *ZSR* isomer fits the experimental VCD better than *ZSS* also in the cluster spectra (Supporting Information, Figure S9).

We have also tested the effect of adding the Grimme empirical dispersion correction[64] in geometry optimizations of SynOxA conformers (CPCM-D_{BS2} geometries). This leads to changes in the relative conformer ordering, resulting in a preference for two structures exhibiting a dispersion interaction between the oxazolidinone ring and the guanidine group (Supporting Information, Figure S10). Averaging over CPCM-D_{BS2} geometries on the basis of the $CPCM_{BS2}$ Boltzmann distribution results in a similar VCD spectrum as for $CPCM_{BS2}$, whereas averaging on the basis of the CPCM-D_{BS2} Boltzmann distribution changes the spectrum significantly, resulting in very poor agreement with experiment (Supporting Information, Figure S11). Although the relative ordering of the dispersion-corrected geometries might be valid for isolated molecules, in solution the intramolecular dispersion interaction is probably weakened by the presence of solvent molecules.

As an alternative to the visual comparison of VCD spectra, we have also compared relative recorded and computed intensities of the VCD bands (Supporting Information, Table S2 and S3). The theoretical spectra with best fit with experiment are employed for this analysis, that is, the results computed on the basis of $CPCM_{BS2}$ geometries for spectra in DMSO-d_6 (Figure 7, right) and on the basis of cluster geometries for spectra in CD_3OD (Figure 8 and Supporting Information, Figure S9). Experimentally, with respect to the most intense band in the spectrum in DMSO-d_6 (1334 cm^{-1}), the relative intensities of the other main peaks are 0.60 (1729 cm^{-1}), 0.65 (1432 cm^{-1}), and 0.85 (1265 cm^{-1}). The respective computed values are 0.70 (1746 cm^{-1}), 0.61 (1425 cm^{-1}), and 0.81 (1269 cm^{-1}) for *ZSR* (Supporting Information, Table S2). These are clearly better than the values of 1.10 (1745 cm^{-1}), 1.35 (1429 cm^{-1}), and 0.76 (1266 cm^{-1}) for *ZSS* (Supporting Information, Table S2). For the spectrum in CD_3OD, the relative intensities between the most intense band (1351 cm^{-1}) and other main peaks are 0.49 (1717 cm^{-1}), 0.62 (1383 cm^{-1}), and 0.66 (1268 cm^{-1}); the respective computed values are 0.38 (1703 cm^{-1}), 0.30 (1424 cm^{-1}), and 0.54 (1271 cm^{-1}) for *ZSR* and 0.24 (1703 cm^{-1}), 0.36 (1414 cm^{-1}), and 0.01 (1263 cm^{-1}) for *ZSS* (Supporting Information, Table S3). Again, *ZSR* provides a significantly better fit.

In summary, we obtain a good agreement between the experimental VCD spectra and the computed spectra for the *ZSR* and *ZSS* isomers of SynOxA. The theoretical spectra for these epimers exhibit some similarities; however, the relative intensities of the main bands and analysis of minor spectral features favor the *ZSR* isomer (Figure 7 and Supporting Information, Table S2 and S3). On basis of these results (as well as the NMR and ROA results above), the absolute configuration of SynOxA can be assigned as (6*Z*,10*S*,11*R*). The C-11 assignment, however, must be considered tentative because of the limitations of the VCD experiment.

Chiroptical AC Assignment of SynOxC. The SynOxC molecule was obtained from the same organism as SynOxA and is likely to be a derivative of SynOxA, generated through

dx.doi.org/10.1021/jo201598x | *J. Org. Chem.* 2012, 77, 858−869

formation of a covalent bond between C-13 and N-9 (Figure 1). A chiroptical analysis of SynOxC can thus provide additional information about the absolute configuration of the synoxazolidinones. On the basis of the above results for SynOxA, the SynOxC molecule is predicted to exhibit a (*Z*)-configuration at C-6 and an (*S*) configuration at C-10. It thus remains to determine the configuration at C-11 (which can be (*R*) or (*S*)), and the configuration at C-13 (which has been predicted to be (*R*) on the basis of NMR results[54]). We have measured the IR and VCD spectra of SynOxC and have compared them to the computed conformationally averaged spectra for the four (6*Z*,10*S*,11*R*/*S*,13*R*/*S*)-isomers of SynOxC (abbreviated *ZSSS*, *ZSRS*, *ZSSR*, and *ZSRR*). Also the ECD spectra were computed and compared to experimental results.[54] Preliminary theoretical ROA analysis of SynOxC indicated that the four isomers would produce very similar spectra, and therefore ROA measurements of SynOxC were not performed.

The theoretical ECD spectra for the four SynOxC isomers show an intense positive peak at ~330 nm and a less intense peak at ~220−260 nm (Supporting Information, Figure S12). The previously reported experimental spectrum[54] displays two positive peaks at ~259 and ~304 nm, showing best fit with the theoretical results for the *ZSSR* and *ZSRR* isomers of SynOxC, but also the *ZSSS* isomer is a viable candidate. Therefore, a clear conclusion on the configuration at C-11 and C-13 of SynOxC cannot be made on the basis of the ECD results.

The computed and recorded IR spectra of SynOxC in CD_3OD show good agreement, in particular if the theoretical spectra are corrected for presence of TFA (Supporting Information, Figure S13). The theoretical and experimental VCD spectra in CD_3OD are compared in Figure S14 (Supporting Information). The two epimers *ZSSR* and *ZSRR* both show good agreement with the experimental VCD spectrum, confirming that the chiral center at C-13 has (*R*) configuration. The spectral area around 1350 cm^{-1} is slightly different for these two isomers; however, comparison to the experimental spectrum does not allow clear assignment of C-11. Addition of explicit solvent molecules provides an equally good fit with experimental VCD data for both *ZSSR* and *ZSRR* (Figure 9). The overall results for SynOxC thus confirm the covalent structure of SynOxC (predicted on the basis of NMR),[54] as well as the configuration at C-6 as (*Z*), at C-10 as (*S*), and at C-13 as (*R*). However, additional information on the C-11 center was not obtained.

Very recently, Polavarapu et al. tested the applicability of optical rotation dispersion (ORD), ECD, and VCD for AC determination of compounds with multiple stereocenters, employing Hibiscus and Garcinia acids as test cases.[65] None of these chiroptical methods were able to elucidate the AC of the test molecules unambiguously; however, combination of VCD with either ECD or ORD was able to correctly predict their configurations. Interestingly, also the combination of VCD with the unpolarized IR spectra was able to provide unambiguous assignments. Whereas IR spectra are identical for enantiomers, for epimers they may show significant differences. IR can also be measured with a higher signal-to-noise ratio than VCD. Unfortunately, for SynOxA and SynOxC, the unpolarized spectra (Raman and IR) for the different stereoisomers do not differ significantly and do not provide additional information about the elusive C-11 center (see, e.g., Figure S13, Supporting Information).

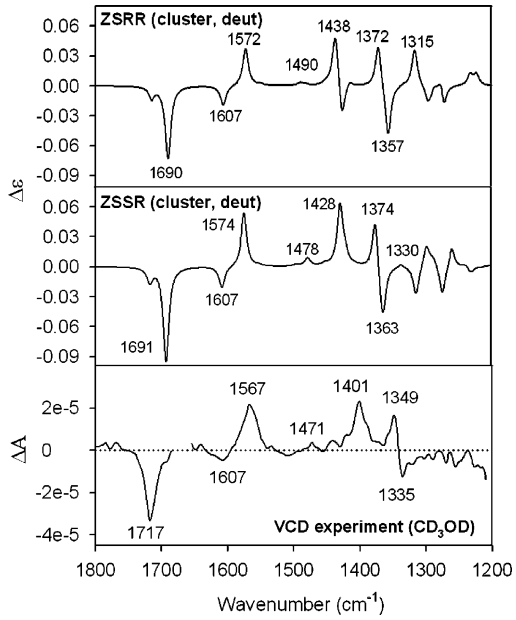

Figure 9. Experimental (CD_3OD) and theoretical VCD spectra for the *ZSRR* and *ZSSR* isomers of SynOxC (averaged over 2 cluster conformers, corrected for deuterium exchange, bandwidth 10 cm^{-1}). The spectral region between 1655 and 1685 cm^{-1} was omitted in the experimental spectrum because of high noise level.

CONCLUSIONS

We have reported a detailed analysis of the ROA, VCD, and ECD chiroptical properties of SynOxA (Figure 1), an antimicrobial oxazolidinone recently isolated from the sub-Arctic ascidian *Synoicum pulmonaria*. SynOxA has two chiral centers (C-10 and C-11) and a double bond with either (*E*)- or (*Z*)-configuration, giving rise to eight possible stereoisomers. The analysis of the spectral parameters of SynOxA was challenged by many different experimental and theoretical difficulties, providing a representative case study for the problems an organic chemist faces when assigning absolute configurations of natural products. The limited amount of the isolated compound did not allow for too extensive spectroscopic studies; in addition, for the VCD analysis, the presence of TFA in the sample caused a strong absorption and prevented a reliable measurement of the VCD signal in the carbonyl spectral region. The flexibility of SynOxA implied that for each isomer as much as 36 conformers had to be included in theoretical calculations of the chiroptical properties. Despite these challenges, a good agreement between the theory and experiment was obtained.

Theoretical and experimental NMR parameters for SynOxA showed good agreement, confirming the experimentally derived covalent structure and further indicating that SynOxA has a (*Z*)-configuration at the double bond between C-6 and C-7. The ECD analysis showed that this technique was able to provide only very limited information on the configuration of SynOxA. The previous AC assignment of SynOxA on the basis of the computed ECD spectra[52] is not supported by our computations. These results stress the importance of employing high-level computational techniques and sufficient conformational sampling for generating theoretical spectra free of spectral artifacts, which potentially can lead to incorrect stereochemical assignments. The recorded and computed ROA spectra provided a reliable assignment of the config-

dx.doi.org/10.1021/jo201598x | J. Org. Chem. 2012, 77, 858−869

uration of SynOxA at the ring stereocenter, which was assigned as (*S*). The double-bond configuration was also evident from ROA, indicating that SynOxA has a (*Z*)-configuration, in agreement with the conclusions drawn from the NMR data. However, the second chiral center of SynOxA at C-11 was silent in the computed ROA. VCD analysis confirmed the (6*Z*,10*S*) assignment made on the basis of ROA; additionally, the configuration at the second chiral center (C-11) could be tentatively assigned as (*R*), resulting in an overall configuration of (6*Z*,10*S*,11*R*). The overall results were further supported by an analysis of the VCD spectra of SynOxC (Figure 1), indicating a (6*Z*,10*S*,11*R*,13*R*) or (6*Z*,10*S*,11*S*,13*R*) absolute configuration for SynOxC.

The chiroptical analysis of the marine compounds SynOxA and SynOxC thus provided a case study of the challenges involved in the determination of the absolute configuration of natural products with multiple stereocenters. Whereas ECD was unable to provide detailed information on the stereochemistry of SynOxA, both ROA and VCD reliably predicted the configuration at C-10 and at the double bond, highlighting the benefits of VOA techniques over electronic methods such as ECD. Furthermore, ROA was unable to resolve the second chiral center of SynOxA, whereas the VCD analysis indicated more specific spectral features for all SynOxA isomers in the theoretical spectra. VCD might therefore be preferable for analysis of similar compounds with multiple stereocenters.

METHODS

Computational Details. All quantum-chemical calculations were performed with Gaussian09.[66] For SynOxA, the eight possible stereoisomers (*ESS*, *ERR*, *ESR*, *ERS*, *ZSS*, *ZRR*, *ZSR*, *ZRS*) were optimized at the B3LYP[67]/6-31+G(d,p)[68]/CPCM(water)[69] level (with cavity generation based on UFF radii scaled by 1.1). For each isomer, 36 local minima with relative enthalpies within 1.5 kcal/mol were obtained (see Supporting Information for further details). To evaluate the effect of the basis set size, dispersion corrections, and explicit solvent molecules, we reoptimized the following SynOxA geometries: (i) all *Z* isomers at the B3LYP/6-311++G(d,p)/CPCM(water) level of theory ($CPCM_{BS2}$ geometries) (ii) the *ZSR* and *ZSS* isomers at the B3LYP/6-311++G(d,p)/CPCM(water) level of theory, including the Grimme empirical dispersion correction (S6 = 1.05,[64] CPCM-D_{BS2} geometries), (iii) the *ZSR* and *ZSS* isomers including 5 explicit water molecules at the B3LYP/6-311++G(d,p)/CPCM(water) level of theory (cluster geometries). The placement of water molecules was identical for all optimized cluster structures and is shown in Figure 2. Six of the CPCM conformers were not stable when adding explicit water molecules, i.e., the total number of SynOxA cluster conformers is reduced to 30. For SynOxC, the *ZSRR*, *ZSSR*, *ZSRS*, and *ZSSS* stereoisomers were optimized at the B3LYP/6-311++G(d,p)/CPCM(water) level of theory. For each isomer, two low-energy conformers were obtained, which differ in the C(1)−O−C(2)−C(3) angle (∼+90° and ∼−90°). All geometries were reoptimized with 3 explicit water molecules coordinated to the carbonyl and guanidinium group.

NMR chemical shifts[70] (including TMS reference) and NMR *J*-coupling constants[71] were computed at the B3LYP/6-311++G(d,p)/CPCM(methanol) level of theory. ECD[72] spectra were simulated on the basis of TD-DFT[73] calculations at both the TD-B3LYP/6-311++G(d,p)/CPCM(methanol) and the TD-LSDA/SVP/CPCM(methanol) level of theory, the latter for comparison to previous results. Raman and ROA[74] spectra were computed at the B3LYP/6-311++G(d,p)/CPCM(water) level with the excitation frequency set to 532 nm. IR and VCD[75] spectra were computed at the B3LYP/6-311++G(d,p)/CPCM(water) level (calculation with DMSO or methanol as solvent resulted in nearly identical spectra). For each isomer, the different spectra and NMR parameters were averaged on the basis of the Boltzmann distribution of the optimized conformers derived from the relative enthalpies (unless otherwise indicated).[76] For the cluster geometries with explicit water molecules, averaging was performed using $CPCM_{BS2}$ Boltzmann distributions (enthalpies of clusters with different hydrogen-bonding patterns could not be used for this purpose). The water signal was removed from all spectra by setting the polarizability derivatives of the solvent atoms to zero.

Experimental Details. SynOxA and SynOxC were isolated with a purity >95% by preparative reverse-phase flash chromatography (Biotage) from a crude acetonitrile extract of a lyophilized sample of *Synochium pulmonaria*. The flash column was a Biotage KP-C18-HS 25+ column, and the eluent was a mixture of water and acetonitrile (both containing 0.1% TFA) with a flow rate of 25 mL/min and UV detection at 254 nm. The identity of the isolated compounds was verified by ESI-MS.

Raman/ROA Spectra. The spectra were measured with the Biotools μ-ChiralRAMAN-2X instrument, equipped with an Opus diode-pumped solid-state laser operating at 532 nm. Raman and ROA spectra were obtained in a fused silica cell with optical path length of 1 mm. SynOxA (∼4 mg) was dissolved in 100 μL of H_2O and bleached via continuous illumination with 500 mW of the 532 nm laser for 1 h. Raman and ROA spectra were acquired using 500 mW laser power at the sample with 2.05 s illumination time for 91 h. Artifact "spikes" (false CCD detector signals, coming from cosmic rays, etc.) were removed.[39] The signal of the solvent was subtracted, and a polynomial baseline correction was applied.

IR/VCD Spectra. The absorption IR and VCD spectra of CD_3OD and DMSO-d_6 solutions of SynOxA and CD_3OD solution of SynOxC were measured using a Bruker IFS66/S FTIR spectrometer equipped with a PMA 37 VCD/IRRAS module (Bruker, Germany). The SynOxA spectra were measured twice from independent samples, employing 5.19 mg SynOxA for the first measurement in CD_3OD and DMSO-d_6 and, respectively, 4.43 and 4.54 mg for the second measurement. For the SynOxC studies, 3.68 mg were used. All samples included the counterion TFA. The approximate concentration of all samples was 0.17 mol L^{-1}. A demountable cell A145 (Bruker, Germany) constructed of CaF_2 windows separated by a 50 μm Teflon spacer was used for all measurements. The spectral resolution was 4 cm^{-1}, and the zero-filling factor was 4. The final spectra were averaged from 21 blocks, each of 2260 interferometric scans accumulated for 20 min. Baseline corrections using the spectra of the relevant solvent obtained under the same conditions were performed.

ASSOCIATED CONTENT

Supporting Information

Additional computational details, absolute energies, coordinates, NMR, ECD, Raman, ROA, IR, and VCD spectra, as referred to in the text. This material is available free of charge via the Internet at http://pubs.acs.org.

AUTHOR INFORMATION

Corresponding Author

*E-mail: kathrin.hopmann@uit.no; bour@uochb.cas.cz.

ACKNOWLEDGMENTS

This work was supported by the Norwegian Research Council through a Centre of Excellence (179568/V30), by a grant of computer time from the Norwegian Supercomputing Program (Notur), Czech Academy of Sciences, Grant Agency of the Czech Republic (P208/11/0105), and the MSMT (LH11033). We thank Dr. Tor Haug for providing us with the raw data for the experimental ECD spectra and Professor Bjørn Gulliksen for providing us with the picture of *Synoicum pulmonaria* (part of the Table of Contents/Abstract graphic).

REFERENCES

(1) Demunshi, Y; Chugh, A *J. Intellect. Prop. Rights* **2009**, *14*, 122−130.

(2) Devlin, F. J.; Stephens, P. J.; Besse, P. *Tetrahedron: Asymmetry* **2005**, *16*, 1557−1566.
(3) Besse, P.; Baziard-Mouysset, G.; Boubekeur, K.; Palvadeau, P.; Veschambre, H.; Payard, M.; Mousset, G. *Tetrahedron: Asymmetry* **1999**, *10*, 4745−4754.
(4) Fietz-Razavian, S.; Schulz, S.; Dix, I.; Jones, P. G. *Chem. Commun.* **2001**, 2154−2155.
(5) Dale, J. A.; Dull, D. L.; Mosher, H. S. *J. Org. Chem.* **1969**, *34*, 2543−2549.
(6) Ohtani, I.; Kusumi, T.; Kashman, Y.; Kakisawa, H. *J. Am. Chem. Soc.* **1991**, *113*, 4092−4096.
(7) Tan, C. H.; Kobayashi, Y.; Kishi, Y. *Angew. Chem. Int. Ed.* **2000**, *39*, 4282−48284.
(8) Taniguchi, T.; Martin, C. L.; Monde, K.; Nakanishi, K.; Berova, N.; Overman, L. E. *J. Nat. Prod.* **2009**, *72*, 430−432.
(9) Allenmark, S. G. *Nat. Prod. Rep.* **2000**, *17*, 145−155.
(10) Dai, J.; Krohn, K.; Flörke, U.; Pescitelli, G.; Kerti, G.; Papp, T.; Kövér, K. E.; Bényei, A. C.; Draeger, D.; Schulz, B.; Kurtán, T. *Eur. J. Org. Chem.* **2010**, 6928−6937.
(11) Guo, Y.-W.; Kurtán, T.; Krohn, K.; Pescitelli, G.; Zhang, W. *Chirality* **2009**, *21*, 561−568.
(12) Cachet, N.; Regaladob, E. L.; Genta-Jouvea, E. L.; Mehiria, M.; Amadea, P.; Thomasa, O. P. *Steroids* **2009**, *74*, 746−750.
(13) Seibert, S. F.; König, G. M.; Voloshina, E.; Raabe, G.; Fleischhauer, J. *Chirality* **2006**, *18*, 413−418.
(14) Polavarapu, P. L. *Chirality* **2008**, *20*, 664−672.
(15) Mukhopadhyay, P.; Zuber, G.; Goldsmith, M.-R.; Wipf, P.; Beratan, D. N. *Chem. Phys. Chem.* **2006**, *7*, 2483−2486.
(16) Aamouche, A.; Devlin, F. J.; Stephens, P. J. *Chem. Commun.* **1999**, 361−362.
(17) Pecul, M. *Chem. Phys. Lett.* **2006**, *418*, 1−10.
(18) Kundrat, M. D.; Autschbach, J. *J. Phys. Chem. A* **2006**, *110*, 12908−12917.
(19) Stephens, P. J.; Pan, J. J.; Devlin, F. J.; Cheeseman, J. R. *J. Nat. Prod.* **2008**, *71*, 285−288.
(20) Kwit, M.; Gawronski, J.; Boyd, D. R.; Sharmab, N. D.; Kaik, M. *Org. Biomol. Chem.* **2010**, *8*, 5635−5645.
(21) Marchesan, D.; Coriani, S.; Forzato, C.; Nitti, P.; Pitacco, G.; Ruud, K. *J. Phys. Chem. A* **2005**, *109*, 1449−1453.
(22) Kwit, M.; Rozwadowska, M. D.; Gawroński, J.; Grajewska, A. *J. Org. Chem.* **2009**, *74*, 8051−8063.
(23) Alagona, G.; Ghio, C.; Monti, S. *Theor. Chem. Acc.* **2007**, *117*, 793−803.
(24) Shcherbin, D.; Ruud, K. *Chem. Phys.* **2008**, *349*, 234−243.
(25) Kundrat, M. D.; Autschbach, J. *J. Phys. Chem. A* **2006**, *110*, 4115−4123.
(26) Diederich, C.; Grimme, S. *J. Phys. Chem., A* **2003**, *107*, 2524−2539.
(27) Atkins, P. W.; Barron, L. D. *Mol. Phys.* **1969**, *16*, 453−466.
(28) Barron, L. D.; Buckingham, A. D. *Mol. Phys.* **1971**, *20*, 1111−1119.
(29) Barron, L. D.; Bogaard, M. P.; Buckingham, A. D. *J. Am. Chem. Soc.* **1973**, *95*, 603−605.
(30) Hug, W.; Kint, S.; Bailey, G. F.; Scherer, J. R. *J. Am. Chem. Soc.* **1975**, *97*, 5589−5590.
(31) Holzwarth, G.; Hsu, E. C.; Mosher, H. S.; Faulkner, T. R.; Moscowitz, A. *J. Am. Chem. Soc.* **1974**, *96*, 251−252.
(32) Nafie, L. A.; Cheng, J. C.; Stephens, P. J. *J. Am. Chem. Soc.* **1975**, *97*, 3842−3843.
(33) Stephens, P. J.; McCann, D. M.; Devlin, F. J.; Smith, A. B. III. *J. Nat. Prod.* **2006**, *69*, 1055−1064.
(34) Costante, J.; Hecht, L; Polavarapu, P. L.; Collet, A.; Barron, L. D. *Angew. Chem. Intl . Ed. Engl.* **1997**, *36*, 885−887.
(35) Lovchik, M. A.; Fráter, G.; Goeke, A.; Hug, W. *Chem. Biodiversity* **2008**, *5*, 126−139.
(36) Wilen, S. H.; Qi, J. Z.; Williard, P. G. *J. Org. Chem.* **1991**, *56*, 485−487.
(37) Stephens, P. J.; Pan, J. J.; Devlin, F. J.; Krohn, K.; Kurtán, T. *J. Org. Chem.* **2007**, *72*, 3521−3536.
(38) Marcos Batista, J. Jr.; Batista, A. N. L.; Rinaldo, D.; Vilegas, W.; Cass, Q. B.; Bolzani, V. S.; Kato, M. J.; López, S. N.; Furlan, M.; Nafie, L. A. *Tetrahedron: Asymmetry* **2010**, *21*, 2402−2407.
(39) Sebestík, J.; Bouř, P *J. Phys. Chem. Lett.* **2011**, *2*, 498−502.
(40) Hopmann, K. H.; Ruud, K.; Pecul, M.; Kudelski, A.; Dračínský, M.; Bouř, P. *J. Phys. Chem. B* **2011**, *115*, 4128−4137.
(41) Kapitán, J.; Johannessen, C.; Bouř, P.; Hecht, L.; Barron, L. D. *Chirality* **2009**, *21*, E4−E12.
(42) Weymuth, T.; Jacob, C. R.; Reiher, M. *Chem. Phys. Chem.* **2011**, *12*, 1165−1175.
(43) Jacob, C. R.; Luber, S.; Reiher, M. *Chem.—Eur. J.* **2009**, *15*, 13491−13508.
(44) Barron, L. D.; Zhu, F.; Hecht, L. *Vib. Spectrosc.* **2006**, *42*, 15−24.
(45) Yaffe, N. R.; Almond, A.; Blanch, E. W. *J. Am. Chem. Soc.* **2010**, *132*, 10654−10655.
(46) Yamamoto, S.; Watarai, H.; Bouř, P. *Chem. Phys. Chem.* **2011**, *12*, 1509−1518.
(47) Profant, V.; Safarik, M.; Bouř, P.; Baumruk, V. *Spectroscopy* **2010**, *24*, 213−217.
(48) Kaminský, J.; Kapitán, J.; Baumruk, V.; Bednárová, L.; Bouř, P *J. Phys. Chem. A* **2009**, *113*, 3594−3601.
(49) Bouř, P.; Sychrovský, V.; Maloň, P.; Hanzlíková, J.; Baumruk, V.; Pospíšek, J.; Buděšínský, M. *J. Phys. Chem. A* **2002**, *106*, 7321−7327.
(50) Pecul, M. *Chem. Phys. Lett.* **2006**, *427*, 166−176.
(51) Nieto-Ortega, B.; Casado, J.; Blanch, E. W.; López Navarrete, J. T.; Quesada, A. R; Ramírez, F. J. *J. Phys. Chem. A* **2011**, *115*, 2752−2755.
(52) Tadesse, M.; Strøm, M. B.; Svenson, J.; Jaspars, M.; Milne, B. F.; Tørfoss, V.; Andersen, J. H.; Hansen, E.; Stensvåg, K.; Haug, T. *Org. Lett.* **2010**, *12*, 4752−4755.
(53) Reference 52 reported best fit between the ECD experiment and theory for the ZSS isomer; however, this conclusion was drawn on the basis of partially mislabeled ECD spectra (see Figure 18 in the Supporting Information of ref 52). The spectra in *red* are the computed spectra, which were correctly labelled. The spectra in *green* are generated by inversion and were incorrectly labelled (for the green spectra, *E* should be *Z*, and *Z* should be *E*). Thus, the theoretical spectrum with best fit is not *ZSS,* but *ESS*.
(54) Tadesse, M.; Svenson, J.; Jaspars, M.; Strøm, M. B.; Abdelrahman, M. H.; Tørfoss, V.; Andersen, J. H.; Hansen, E.; Kristiansen, P. E.; Stensvåg, K.; Haug, T. *Tetrahedron Lett.* **2011**, *52*, 1804−1806.
(55) Dračínský, M.; Bouř, P. *J. Chem. Theory Comput.* **2010**, *6*, 288−299.
(56) Malkin, V. G.; Malkina, O. L.; Salahub, D. R. *Chem. Phys. Lett.* **1996**, *261*, 335−345.
(57) Vaara, J.; Ruud, K.; Vahtras, O.; Ågren, H.; Jokisaari, J. *J. Chem. Phys.* **1998**, *109*, 1212−1222.
(58) Marshall, J. L. *Carbon-Carbon and Carbon-Proton NMR Couplings: Applications to Organic Stereochemistry and Conformational Analysis*; Verlag Chemie Int: Deerfield Beach, FL, 1983.
(59) Crawford, T. D.; Tam, M. C.; Abram, M. L. *Mol. Phys.* **2007**, *105*, 2607−2617.
(60) Elsässer, B.; Krohn, K.; Akhtar, M. N.; Flörke, U.; Kouam, S. F.; Kuigoua, M. G.; Ngadjui, B. T.; Abegaz, B. M.; Antus, S.; Kurtán, T. *Chem. Biodiversity* **2005**, *2*, 799−808.
(61) Jacob, C. R.; Luber, S.; Reiher, M. *ChemPhysChem* **2008**, *9*, 2177−2180.
(62) Zuber, G.; Hug, W. *Helv. Chim. Acta* **2004**, *87*, 2208−2234.
(63) The VCD spectra were recorded in methanol; however, explicit water molecules can be considered to provide a similar hydrogen-bonding pattern as methanol would.
(64) Grimme, S. *J. Comput. Chem.* **2006**, *27*, 1787−1799.
(65) Polavarapu, P. L.; Donahue, E. A.; Shanmugam, G.; Scalmani, G.; Hawkins, E. K.; Rizzo, C.; Ibnusaud, I.; Thomas, G.; Habel, D.; Sebastian, D. *J. Phys. Chem. A* **2011**, *115*, 5665−5673.
(66) Frisch, M. J.; Trucks, G. W.; Schlegel, H. B.; Scuseria, G. E.; Robb, M. A.; Cheeseman, J. R.; Scalmani, G.; Barone, V.; Mennucci, B.; Petersson, G. A.; Nakatsuji, H.; Caricato, M.; Li, X.; Hratchian, H.

P.; Izmaylov, A. F.; Bloino, J.; Zheng, G.; Sonnenberg, J. L.; Hada, M.; Ehara, M.; Toyota, K.; Fukuda, R.; Hasegawa, J.; Ishida, M.; Nakajima, T.; Honda, Y.; Kitao, O.; Nakai, H.; Vreven, T.; Montgomery, J. A.; , Jr., Peralta, J. E.; Ogliaro, F.; Bearpark, M.; Heyd, J. J.; Brothers, E.; Kudin, K. N.; Staroverov, V. N.; Keith, T.; Kobayashi, R.; Normand, J.; Raghavachari, K.; Rendell, A.; Burant, J. C.; Iyengar, S. S.; Tomasi, J.; Cossi, M.; Rega, N.; Millam, J. M.; Klene, M.; Knox, J. E.; Cross, J. B.; Bakken, V.; Adamo, C.; Jaramillo, J.; Gomperts, R.; Stratmann, R. E.; Yazyev, O.; Austin, A. J.; Cammi, R.; Pomelli, C.; Ochterski, J. W.; Martin, R. L.; Morokuma, K.; Zakrzewski, V. G.; Voth, G. A.; Salvador, P.; Dannenberg, J. J.; Dapprich, S.; Daniels, A. D.; Farkas, O.; Foresman, J. B.; Ortiz, J. V.; Cioslowski, J.; Fox, D. J. *Gaussian 09*, Revision B.01;Gaussian, Inc.: Wallingford, CT, 2010.

(67) (a) Becke, A. D. *J. Chem. Phys.* **1993**, *98*, 5648−5652. (b) Lee, C.; Yang, W.; Parr, R. G. *Phys. Rev. B* **1988**, *37*, 785−789.

(68) (a) McLean, A. D.; Chandler, G. S. *J. Chem. Phys.* **1980**, *72*, 5639−5648. (b) Raghavachari, K.; Binkley, J. S.; Seeger, R.; Pople, J. A. *J. Chem. Phys.* **1980**, *72*, 650−654. (c) Binning, R. C. Jr.; Curtiss, L. A. *J. Comput. Chem.* **1990**, *11*, 1206−1216. (d) McGrath, M. P.; Radom, L. *J. Chem. Phys.* **1991**, *94*, 511−516. (e) Curtiss, L. A.; McGrath, M. P.; Blaudeau, J.-P.; Davis, N. E.; Binning, R. C. Jr.; Radom, L. *J. Chem. Phys.* **1995**, *103*, 6104−6113.

(69) (a) Barone, V.; Cossi, M. *J. Phys. Chem. A* **1998**, *102*, 1995−2001. (b) Cossi, M.; Rega, N.; Scalmani, G.; Barone, V. *J. Comput. Chem.* **2003**, *24*, 669−681.

(70) (a) Gauss, J. *Ber. Bunsenges. Phys. Chem.* **1995**, *99*, 1001−1008. (b) Cheeseman, J. R.; Trucks, G. W.; Keith, T. A.; Frisch, M. J. *J. Chem. Phys.* **1996**, *104*, 5497−5509.

(71) (a) Helgaker, T.; Watson, M.; Handy, N. C. *J. Chem. Phys.* **2000**, *113*, 9402−9409. (b) Sychrovsky, V.; Gräfenstein, J.; Cremer, D. *J. Chem. Phys.* **2000**, *113*, 3530−3547. (c) Barone, V.; Peralta, J. E.; Contreras, R. H.; Snyder, J. P. *J. Phys. Chem. A* **2002**, *106*, 5607−5612. (d) Peralta, J. E.; Scuseria, G. E.; Cheeseman, J. R.; Frisch, M. J. *Chem. Phys. Lett.* **2003**, *375*, 452−458. (e) Deng, W.; Cheeseman, J. R.; Frisch, M. J. *J. Chem. Theory Comput.* **2006**, *2*, 1028−1037.

(72) (a) Bak, K. L.; Jørgensen, P.; Helgaker, T.; Ruud, K.; Jensen, H. J. A. *J. Chem. Phys.* **1993**, *98*, 8873−8887. (b) Bak, K. L.; Hansen, A. E.; Ruud, K.; Helgaker, T.; Olsen, J.; Jørgensen, P. *Theor. Chem. Acc.* **1995**, *90*, 441−458. (c) Olsen, J.; Bak, K. L.; Ruud, K.; Helgaker, T.; Jørgensen, P. *Theor. Chem. Acc.* **1995**, *90*, 421−439. (d) Hansen, A. E.; Bak, K. L. *Enantiomer* **1999**, *4*, 455−476. (e) Autschbach, J.; Ziegler, T.; van Gisbergen, S. J. A.; Baerends, E. J. *J. Chem. Phys.* **2002**, *116*, 6930−6940.

(73) (a) Bauernschmitt, R.; Ahlrichs, R. *Chem. Phys. Lett.* **1996**, *256*, 454−464. (b) Casida, M. E.; Jamorski, C.; Casida, K. C.; Salahub, D. R. *J. Chem. Phys.* **1998**, *108*, 4439−4449. (c) Stratmann, R. E.; Scuseria, G. E.; Frisch, M. J. *J. Chem. Phys.* **1998**, *109*, 8218−8224. (d) Van Caillie, C.; Amos, R. D. *Chem. Phys. Lett.* **1999**, *308*, 249−255. (e) Van Caillie, C.; Amos, R. D. *Chem. Phys. Lett.* **2000**, *317*, 159−164. (f) Furche, F.; Ahlrichs, R. *J. Chem. Phys.* **2002**, *117*, 7433−7447. (g) Scalmani, G.; Frisch, M. J.; Mennucci, B.; Tomasi, J.; Cammi, R.; Barone, V. *J. Chem. Phys.* **2006**, *124*, 1−15.

(74) (a) Helgaker, T.; Ruud, K.; Bak, K. L; Jørgensen, P.; Olsen, J. *Faraday Discuss.* **1994**, *99*, 165−180. (b) Dukor, R. K.; Nafie, L. A. In *Encyclopedia of Analytical Chemistry: Instrumentation and Applications*; Meyers, R. A., Ed.; Wiley & Sons: Chichester, 2000; pp 662−676. (c) Ruud, K.; Helgaker, T.; Bour, P. *J. Phys. Chem. A* **2002**, *106*, 7448−7455. (d) Barron, L. D. *Molecular Light Scattering and Optical Activity*, 2nd ed.; Cambridge University Press: Cambridge, U.K., 2004. (e) Thorvaldsen, A. J.; Ruud, K.; Kristensen, K.; Jørgensen, P.; Coriani, S. *J. Chem. Phys.* **2008**, *129*, 214108.

(75) (a) Cheeseman, J. R.; Frisch, M. J.; Devlin, F. J.; Stephens, P. J. *Chem. Phys. Lett.* **1996**, *252*, 211−220. (b) Coriani, S.; Thorvaldsen, A. J.; Kristensen, K.; Jørgensen, P. *Phys. Chem. Chem. Phys.* **2011**, *13*, 4224−4229.

(76) Computation of entropy (and hence Gibbs Free energies) can be rather unreliable and averaging over the enthalpies is therefore preferred. However, we have tested the effect of averaging over the Gibbs Free energies as well and find that the resulting ECD, ROA, and VCD spectra look almost identical.